Materials Science-Poland, 30(1), 2012, pp. 53-62
http://www.materialsscience.pwr.wroc.pl/
DOI: 10.2478/s13536-012-0005-4

VERSITA

Carbon Microflowers*

A. T. SOBCZYK[1], A. JAWOREK[1,2†], Z. SOBISZ[3]

[1]Institute of Fluid Flow Machinery, Polish Academy of Sciences, Fiszera 14, 80-952 Gdansk, Poland

[2]Institute of Physics, Pomeranian Academy, Arciszewskiego 22B, 76-200 Słupsk, Poland

[3]Institute of Biology and Environment Protection, Pomeranian Academy, Arciszewskiego 22B, 76-200 Słupsk, Poland

Micro- or nanoflowers are self-organized, planar or 3D microstructures similar to macroscopic flowers. The interest in microflowers has increased in recent years because of many potential applications of microflowers, due to their high specific surface area. The analysis of the morphology of carbon flower-like microstructures produced in low-current plasma, generated by high voltage electrical discharge in a mixture of cyclohexane with argon as the carrier gas has been presented in the paper. It was shown that various carbon microstructures, including microfibers and microflowers of different pattern, can be synthesized on the electrodes by the same plasma method, at various process parameters.

Keywords: *microflower, nanoflower, flower-like, plasma methods, carbon*

1. Introduction

Micro- or nanoflower is a self-organized, highly regular planar or 3D microstructure resembling a macroscopic biological form known as a flower. In recent years, microflowers have drawn a significant attention of scientists not only due to their aesthetic features, but also because of powerful potential applications owing to their high specific surface area. The term ”nanoflower” has been probably used for the first time by Yan Qiu Zhu et al. [1, 2] in their papers published in 1998 and 1999, and ”flower-like” morphology was used by Shi et al. in 1994 [3], although ”cauliflower-like” structures were mentioned in many earlier papers.

Microflowers can be formed by using standard ”bottom-up” methods applied in microfabrication or in nanotechnology, and built from almost all metal, ceramic or polymer materials as an incomplete growth of a bulk product. The techniques used for microflowers synthesis include, for example, oxidation of elemental metals, reduction of metal salts, thermal decomposition of relatively unstable compounds, electrochemical or plasma decomposition [4, 5]. Because each flower has its own structure and two of them are not identical (like two snowflakes) the process of microflower building cannot be exactly reproducible. However, the general form of a structure remains the same for the same material and formation at the same process conditions.

Although the number of publications devoted to micro- or nanoflowers has increased exponentially in the last decade, the carbon structures, declared by the authors as carbon micro- or nanoflowers (or flower-like structures) can be met only in the few ones.

*This paper was presented at the Conference Functional and Nanostructured Materials, FNMA 11, 6-9 September 2011, Szczecin, Poland

†E-mail: jaworek@imp.gda.pl

Table 1. Summary of the methods used for carbon microflower synthesis.

Reference	**Method**	**Precursor /Atmosphere**	**Substrate /Catalyst**	**Process parameters**	**Characteristics**
Charinpanitkul et al. [10]	arc discharge	cryogenic nitrogen	graphite–graphite, or iron–graphite electrodes	75 – 150 A, 16.5 – 44.0 kW, 3 min, arc power efficiency 60 – 84%, 4800 K	single-walled carbon nanohorns and multi-walled nanoflowers 100 – 200 nm dia. (graphite), 70 – 120 nm (iron)
Chuang et al. [25]	microwave plasma-enhanced chemical vapor deposition	$C_2H_2 + NH_3$	silicon substrates, without metal catalyst	10 min, 500 W, 1.33 kPa	nanowalls, 30 – 50 nm thick,
Deng et al. [8]	microwave plasma chemical vapor deposition	$CH_4 + H_2$	ceramic substrates, Fe–Ni–Cr catalyst	6 kPa, 700 °C, 1600 kW, 100 sccm (H_2), 8 sccm CH_4, 10 min	nano-crystalline graphite slices 10 nm thick
Donnet et al. [26]	combustion in oxygen /acetylene flame	$C_2H_2 + O_2$ (1.68 and 1.3 slm)	carbon black substrate	1 min, 1200 – 1700 °C, >atmospheric pressure	MWCNTs 10 – 20 nm dia., 50 μm long
Du et al. [13]	reduction–pyrolysis–catalysis	glycerin	magnesium reductant and ferrocene catalyst	650 °C pyrolysis, 50 °C for 10 h drying in vacuum, yield of carbon 80%	graphitic feature, sphere-shaped network structure 300 – 400 nm dia. with lots of flakes 5 nm thick, hollow core diameter 200 – 600 nm
Krivchenko et al. [9]	dc glow discharge	$CH_4 + H_2$ (3:97 to 8:92)	Si (100)	substrate treated with microwave discharge in 805 ° C and 850 °C with $CH_4 + H_2$ in low pressure, 6.66 kPa to 26.6 kPa after discharge ingnition	carbon nanosheet (nanowalls)
Lisi et al. [6]	hot filament chemical vapor deposition	CH_4 + He (2:98)	carbon fibers	substrate: 700 °C filament: 2200 °C, gas: 100 sccm, 30 mbar	carbon nanosheets (nanowalls)

Ma et al. [27]	catalytic chemical vapor deposition	toluene + argon	ferrocene catalyst	1000 – 1200 °C, 150 – 2500 ml/min (Ar), 30 – 90 min	fiber lengths of several centimeters and diameters of 2 – 10 mm, branch diameter 5 – 10 μm, graphite nodules
Ma and Yuan [11]	plasma-enhanced chemical vapor deposition	CH_4 + H_2 + Ar 1:3:3 to 1:3:6 (by vol.)	Si (1 1 1) substrate, Fe catalyst	50 – 300 Pa, 500 W, 500 V, 2 – 4 h, 500–650 °C	2D carbon nanoflowers: nanoleaves 6.5 nm thick, 2.5 μm long, 250 nm wide; 3D nanoflowers: hundreds of nanofibers 30 nm dia., 0.5 – 0.8 μm long, corolla 6.5 μm dia. 40% porosity, hexagonal graphite
Mukhopadhyay and Rao [4]	catalytic chemical vapor deposition	C_2H_2 + H_2 + N_2	nickel sulphide catalyst (powder)	500 ml/min (C_2H_2), 300 ml/min (H_2), 200 ml/min (N_2), 850 °C	95% purity, crystalline structure, 300 – 400 m^2/g, 2 – 10 mg/cm^3, 5 nm pores
Qiu et al. [28]	arc discharge	coal-based carbon (anode), graphite (cathode), C_2H_2 + H_2 (1:5 vol.)	Fe catalyst	50 – 60 A, 40 – 50 V, 60 – 65 kPa, 5 – 7 min	carbon fibers 100 – 150 μm dia., 1.2 – 1.5 μm, graphite crystallites (building blocks)
Sharma et al. [29]	sol–gel poly-conden-sation, inverse emulsification in cyclohexane containing non-ionic surfactant, pyrolysis in N_2	resorcinol with formaldehyde in alkaline aqueous solution + surfactant (1 – 4 vol.%)	quartz substrate, potassium carbonate catalyst	1 – 2 h stirring, 1173 K calcination	microspheres 5 – 46 μm dia., amorphous carbon
Shih et al. [30]	RF sputtering	Ar + CH_4 + H_2 10:0:0 to 10:5:10	Si (100)	300 – 450 ° C, 1 Pa	nanoflakes

Tang et al. [31]	chemical vapor deposition	camphor ($C_{10}H_{16}O$) in Ar	ferrocene catalyst	500 – 2500 ml/min (Ar), 1000 – 1150 °C	carbon microspheres (building blocks)
Thongtem et al. [7]	thermal decomposition	C_2H_2 + Ar	glass slides substarte, iron dots (1 μm) as catalyst	700 – 900 K, 300 s, 10^5 Pa, 2.14×10^{-2} μm/s growth rate, 10 ml/s (Ar), 0.1 ml/s (C_2H_2)	hexagonal structure
Wang et al. [32]	radio-frequency plasma enhanced chemical vapor deposition	CH_4+H_2 (5:95 to 100:0)	Si, SiO_2, Al_2O_3, Mo, Zr, Ti, Hf, Nb, W, Ta, Cu and 304 stainless steel	600 – 900 °C	carbon nanosheets (nanowalls)
Wang et al. [33]	microwave plasma enhanced chemical vapor deposition	CH_4 + Ar (1:8)		450 °C, 17.3 Pa	carbon nanosheets (nanowalls)
Xiao et al. [34]	solvothermal method	$Mg(CH_3COOH)_2\cdot 4H_2O$ + 10 ml of polyethylene glycol		600 °C calcination, (10 °C/min ramp), 24 h	flowers 8 – 10 μm dia. made of flakes, hexagonal crystalline carbon
Xu et al. [35]	self-assembly template		quartz substrate, ferrocene catalyst	600 °C, 16 h	hollow, amorphous or hexagonal graphite, or cnt 25 – 200 nm dia., 10 – 15 nm wall thickness
Zhang et al. [12]		ethylene (99.95%), 95% Ar (99.999%), 5% H_2 (99.999%)	ethylene or ceramic spheres substrate	800 °C, 800 sccm (Ar+H_2), 1.0 nm/min growth rate	aligned CNTs 10 nm in. dia., 23 nm out.dia. (mean), identical length 1100 nm, uniform orientation

Carbon micro-flowers were produced, for example, using catalytic chemical vapour deposition technique from acetylene on nickel sulphide catalyst [4, 6], on iron dots as a catalyst by thermal decomposition of C_2H_2 in Ar at a temperature ranging from 700 to 900 K [7], by microwave plasma chemical vapor deposition on Fe–Ni–Cr catalyst from CH_4 [8, 9], by arc discharge in cryogenic nitrogen from graphite [10], by plasma-enhanced chemical vapor deposition, using CH_4 in H_2 and Ar on Fe catalyst [11], from ethylene, cyclohexane or LPG [12], or from glycerin by reduction–pyrolysis–catalysis processes using magnesium and ferrocene as reductant and catalyst, respectively [13]. The specific surface area of carbon microflowers can

be as high as 300 – 400 m^2/g, with adsorption average pore diameter about 5 nm [4]. The details of process parameters of various methods used for carbon microflower synthesis are summarized in Table 1.

Carbon microflowers can potentially be used for hydrogen storage, as electrode material for fuel cells, supercapacitors, solar cells, cathodes for field emission displays, as filler for polymers or nanocomposites, or as electromagnetic energy absorbers. The carbon microflowers were built from MWCNTs, carbon fibers, platelets or graphenes. Although the forms of carbon microflowers have not been classified yet, some regular features in these structures can be observed. Carbon microstructures, mainly in the graphene or CNT forms, were also used as a substrate for building other nano- or microflowers from various materials, for example, Pt as catalyst, [14, 15] or ZnO as an electrochemiluminescent device [16].

In this paper we have analyzed the morphology of carbon flower-like microstructures produced in low-current plasma, generated by high voltage electrical discharge in a mixture of cyclohexane with argon as the carrier gas [17–19].

2. Experimental

The method of carbon structures production in electrically generated plasma is based on the decomposition of hydrocarbon vapours in oxygen-free gaseous atmosphere usually at atmospheric pressure and at room temperature. The plasma was generated by high voltage electrical discharge of positive polarity ranging from 5 to 25 kV, by keeping the discharge current at the level of 0.1 to 3 mA. The discharge was generated between a needle discharge electrode (diameter of 1 mm, stainless steel, elemental composition of Fe+Cr+Ni) and a plate (24×40 mm, stainless steel, elemental composition Ni+Fe+Mo as is illustrated in Fig. 1). The distance between the electrodes was 15 mm. The discharge electrodes were supplied from high voltage DC source SPELLMAN HV SL 600W/40kV/PN of positive polarity. A ballast resistance of 5 MOhm was connected between the discharge electrode and HV supply unit in order to limit the discharge current. The reactor chamber of the volume of 0.1 L was made of PMMA. Gas mixture of cyclohexane C_6H_{12} as carbon precursor in carrier gas Ar, with the concentration ranging from 1 to 5 at.% and at near atmospheric pressure was used for the formation of the carbon microstructures. The flow rate of the gas mixture was 0.08 L/min. The process was carried out at ambient temperature.

The physical properties of the carbon structures were determined using scanning electron microscopy (SEM, Zeiss EVO 40), energy dispersive spectroscopy (EDS, Bruker Quantax 400 with detector SDD X-flash 5010, 10 mm^2, 125 eV), Raman spectroscopy (Renishaw inVia Raman Microscope with a 100× objective lens and a laser with the wavelength of 785 nm and power of 1.5 mW), and X-ray diffraction analysis (Phillips X'Pert system with Cu Kα radiation).

3. Results

Typical photographs of the discharge for positive polarity in Ar:C_6H_{12} mixture (1-5 at.%) before synthesis of the carbon structure, i.e., just after switching-on the voltage (a) and after 5 s of the synthesis of the carbon microstructures upon the discharge and plate electrodes (b) are shown in Fig. 2. In these photographs, the needle electrode is at the top of the figure and the grounded plate is placed beneath. The bright point at the top of Fig. 2a is the ionization zone at the needle tip. The bright point shifts downwards with the growth of carbon fiber (Fig. 2b), and now, the ionization zone is at the tip of the carbon fiber growing from the tip of the needle electrode (not visible). The bright region in the bottom of the figure is due to the discharge processes at the carbon microstructures grown on the plate electrode. The bluish zone between the electrodes is the plasma column formed by the ionised Ar atoms.

Depending on the process parameters, such as carbon feedstock and its concentration, kind of carrier gas, reaction temperature, supply voltage, discharge current, material of the electrodes,

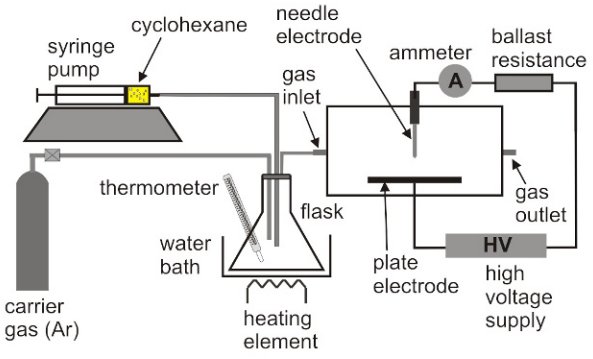

Fig. 1. Schematic of experimental set-up for the production of carbon microstructures.

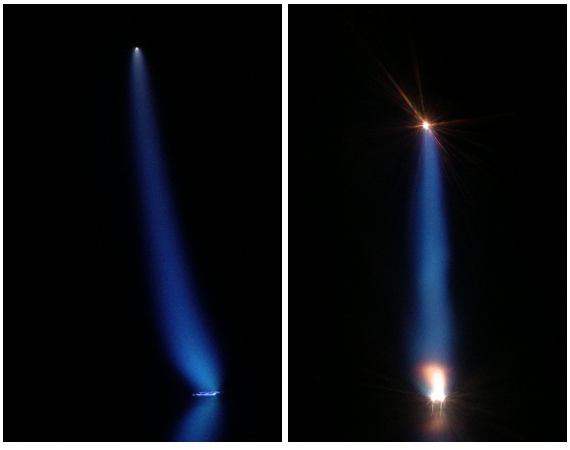

(a) (b)

Fig. 2. Photographs of the discharge in Ar:C_6H_{12} (4 at.%) gas mixture for positive polarity; (a) discharge just after switching-on the voltage, (b) discharge during the synthesis of the carbon structures (1/100 s); discharge current: 1.8 mA, voltage drop between the electrodes: 2.25 kV.

distance between the electrodes, time of synthesis, various carbon structures have been built on the electrodes. However, there is a lack of general rules of the effect of these process parameters on the carbon structures formation. In the particular case of C_6H_{12} in Ar, presented in this paper, the synthesized carbon structures of different morphology, size and shape are shown in Fig. 3, for the discharge current increasing from 0.6 to 3 mA. For the current ranging from 1.4 to 3 mA, oblong forms, which can be considered as carbon fibers, have been synthesised at the tip of the needle electrode. The diameter of the fibers can range from about 20 μm to 70 μm, and their length from 1 to 12 mm, depending on the current, during 30 s synthesis process. For a constant discharge current (for example, 1.8 mA), but different C_6H_{12} concentration, fibers of different morphologies were obtained: columnar structures with cauliflower-like surface, for 1 – 2 at.% (a, b), or the smooth ones, for 3 – 5 at.% (c, d). The carbon structures deposited at 1 – 2 at.% of cyclohexane concentration had fractal morphology, which could be attributed to the way of their growth. According to the literature, it is supposed that such a microstructure grows mainly by the diffusion-limited aggregation rather than ballistic deposition [20]. In a diffusion-limited growth process, the deposition rate depends only on the flux of reactive species and the product is characterized by the fractal shape [21, 22]. For higher cyclohexane concentration (3 – 5 at.%), the layer-by-layer amorphous carbon growth takes place (cf. Fig. 3d). The mean power of discharge was in the range of 1 – 6 W.

Other carbon structures formed at the needle tip or at the plate electrode, at various process parameters, and their arbitrarily selected flower counterparts are shown in Fig. 4. For aesthetic reasons the produced microflowers were referred to the actual biological species. The shape and size of the deposited carbon structures strongly depend on the precursor concentration and the discharge current.

An example of the Raman spectrum of carbon products is shown in Fig. 5. The Raman spectrum in the range from 1000 to 1700 cm^{-1} has the following peaks: 1192 cm^{-1}, 1309 cm^{-1}, 1486 cm^{-1} and 1598 cm^{-1}, corresponding to carbon D- and G-bands, which indicate hexagonal graphite-lattice structure and the existence of large quantity of carbonaceous impurities. The 1192 cm^{-1} band is uncertain, it could be due to sp^3 C-C stretching vibrations, C-H bonds, or mixed sp^2-sp^3 bonds.

X-ray diffraction measurements shown in Fig. 6 indicate that the carbon structures obtained

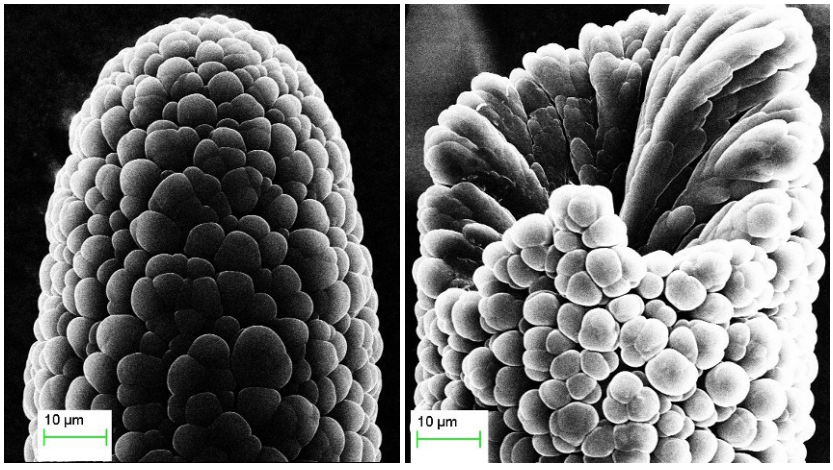

(a) Tip of porous carbon fiber (b) Fracture of porous carbon fiber

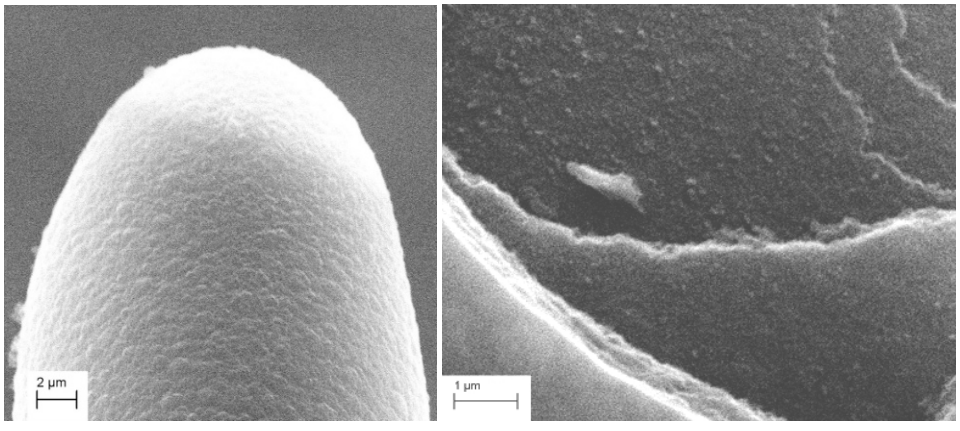

(c) Tip of smooth carbon fiber (d) Fracture of smooth carbon fiber

Fig. 3. SEM micrographs of carbon microfibers synthesised at the tip of the discharge electrode. Time of the synthesis of carbon structures: for (a) and (b) - 10 min, C_6H_{12} concentration - 1 at.%, and for (b) and (c) 30 s, C_6H_{12} concentration - 5 at.%; discharge current - 1.8 mA, voltage between the electrodes about 1 kV.

during the discharge were partially crystalline and partially amorphous. The 2θ peaks at 25.2°, 27.5°, 28.4°, 30°, 32.3°, 33.41°, 41°, 47.5° were recorded. The XRD peak at 2θ = 25.2° and/or a broad peak from 23° to 27° could correspond to the (002) plane of graphite. The peak shifts and peak broadening could be an effect of surface curvature and disordered stacking of graphene layers [23]. Diffraction angles at 2θ = 28.4° and 47.5° correspond to Si (sample holder of XRD system). The peaks at 27.5°, 30°, 32.3°, 33.41°, 41° marked with asterisks correspond to other not identified crystalline components in the sample.

The elemental analysis was used to identify atomic percentage of carbon and hydrogen in the synthesized deposit. The analysis confirmed that carbon is the dominant element in the product, with C – 89.9 at.% and H – 9.8 at.%, the rest was N and O absorbed from the atmosphere (comparing to cyclohexane of C – 33.33 at.% and H – 66.66 at.%). It is therefore evident that highly carbonised products can be obtained by the decomposition of cyclohexane in electrically generated plasma.

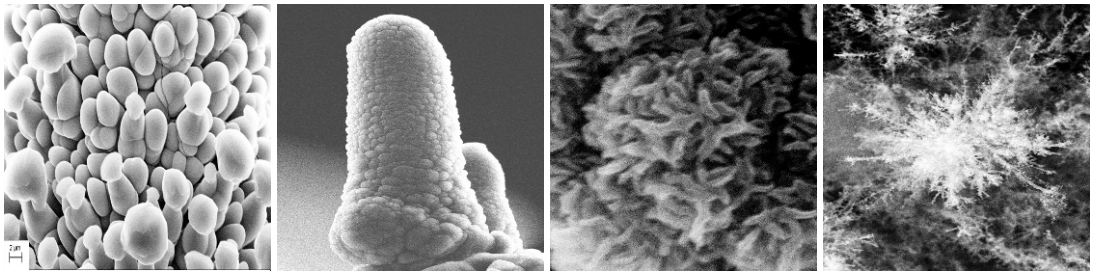

(a) i=1.8 mA, t=30 s Ar + C_6H_{12} (1 at.%)
(b) i=1.4 mA, t=30 s Ar + C_6H_{12}(4 at.%)
(c) i=1.4 mA, t=30 s Ar + C_6H_{12} (5 at.%)
(d) i=3 mA, t=30 s Ar + C_6H_{12} (5 at.%)

(e) Parrot's beak *(Heliconia psittacorum)*
(f) Crepe ginger *(Costus speciosus)*
(g) Jungle flame *(Ixora coccinea)*
(h) Red peacock *(Brassica oleracea)*

Fig. 4. Carbon microstructures and their flower-counterparts (photograph h: www.jungleseeds.com/SeedShop).

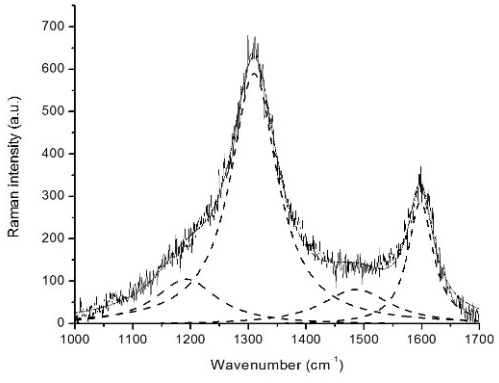

Fig. 5. Raman spectrum of carbon microstructures (solid line: experimental, dashed line: results of deconvolution) (discharge current i = 1.8 mA, voltage U = 1 kV, concentration 4 at.% C_6H_{12}).

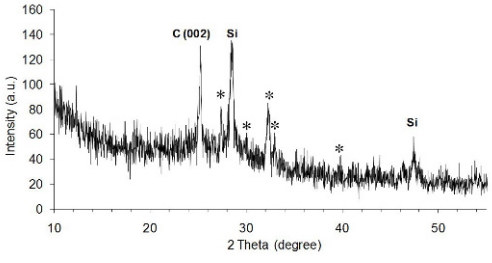

Fig. 6. X-ray diffraction measurements of carbon microstructures (discharge current i = 1.8 mA, voltage U = 1 kV, concentration 4 at.% C_6H_{12}).

4. Discussion

Pyrolytic decomposition of gas-phase precursors takes place in the plasma column at the following stages: The primary decomposition, providing free radicals with a very short life time, which recombine to form unsaturated aliphatic species. Next, by dehydrogenation, cyclisation, and the addition of radicals, followed by aromatisation and polycondensation reactions, the unsaturated aliphatic species can be transformed into polycyclic aromatic hydrocarbons [24]:

$$
\begin{aligned}
& c - C_6H_{12} + e \rightarrow R^{\bullet}_m + R^{\bullet}_n \\
& c - C_6H_{12} + Ar_m \rightarrow Ar\left({}^1S_0\right) + R^{\bullet}_m + R^{\bullet}_n \\
& c - C_6H_{12} + H^* \rightarrow R^{\bullet}_m + \text{neutral products} \\
& R^{\bullet}_n \rightarrow P_l + R^{\bullet}_{n-l} \\
& R^{\bullet}_x + R^{\bullet}_y \rightarrow P_{x+y}
\end{aligned}
$$

where Ar_m is argon in metastable state, R_z is a radical produced during the discharge due

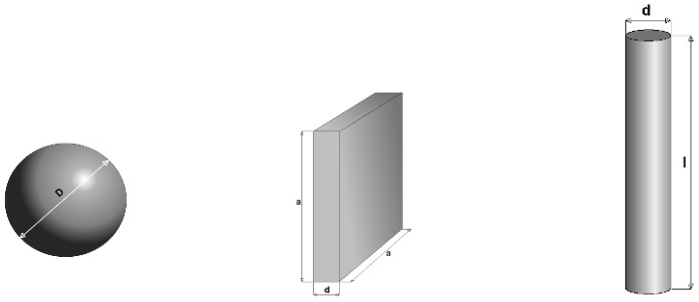

(a) spherical particle $S = \pi D^2$; $V = \frac{\pi}{6} D^3$ specific surface area $(S/m)_{\text{sphere}} = \frac{\pi D^2}{m}$

(b) petal $S = 4ad + 2a^2$; $V = a^2 d$ specific surface area (d=D/10, V=Vsphere) $(S/m)_{\text{petal}} = 3.6 \times (S/m)_{\text{sphere}}$

(c) whisker $S = \frac{\pi}{2} d^2 + \pi dl$; $V = \frac{\pi}{4} d^2 l$ specific surface area (d=D/10, V=Vsphere) $(S/m)_{\text{whisker}} = 6.6 \times (S/m)_{\text{sphere}}$

Fig. 7. Comparison of specific surface areas for various building blocks of microflowers.

to dissociation of hydrocarbons (for example, hydrogen atom H*), P_z is a neutral product (hydrocarbon) of higher molecular weight than cyclohexane. Because the atomic carbon is the dominant element in carbon microstructure, it could be supposed that the growth of these structures is due to the addition of atomic carbon or carbon clusters. An example of two such processes leading to the formation of atomic carbon, as an effect of the collision of fast electrons with hydrocarbon molecule, can be as follows:

$$e + C_x H_y \rightarrow C_{x-1} H_{y-2} + H_2 + C + e$$
$$e + C_x H_y \rightarrow C_{x-1} H_{y-2} + H_2 + C^-$$

These processes occur mainly near the needle electrode where the concentration of the electrons is the highest and they gain high energy due to strong electric field in this zone.

It was shown that carbon microflowers obtained in these experiments have partially crystalline and partially amorphous structure (cf. Figs. 5 and 6). Thongtem et al. [7] has obtained, for example, hexagonal structure. Hydrogen found in carbon fiber could result from electronegative products of decomposed cyclohexane, such as CH_2, CH_3, C_2H and C_2H_3, which were adsorbed on the surfaces of previously deposited products during the process of synthesis (cf. the peak at 1192 cm^{-1} in Raman spectra).

It was emphasised in many papers that flower-like microstructures, due to their larger surface to volume (or mass) ratio, are particularly attractive because the performances of the devices based on such structures are significantly higher than those built from conventional spherical nano/microparticles. Specific surface area of a spherical particle covering a substrate can be compared with a flat petal or a cylindrical whisker, as the most frequently met building blocks of microflowers, which are of the same mass (volume and density) as that of the spherical particle (Fig. 7). For a petal of a thickness of 1/10 of the sphere diameter, the specific surface area is 3.6 times higher than that of the sphere, and for a whisker of a diameter of 1/10 of the sphere diameter, this parameter is 6.6 times higher than for the sphere. Although actually these blocks are usually not straight but can be curved or bent, their specific surface area remains approximately the same.

5. Conclusions

The paper showed that various carbon microstructures, including microfibers and microflowers of different shape, can be synthesized on the electrodes by the same plasma method, by various process parameters. In this particular case, high-voltage low-current arc discharge of positive polarity supplied form a high voltage source, with the discharge current in the range from 0.1 to 3 mA was tested as a method of such structures synthesis. The oblong carbon structures

or carbon fibers synthesized at the tip of a needle electrode had the length ranging from 0.5 to 7 mm (limited by the electrodes distance and time of synthesis), and their diameter varied from about 20 to 80 μm, depending on hydrocarbon concentration and the discharge current. Their maximum growth rate was 0.24 mm/s for dense structure, and 0.15 mm/s for porous cone-like structure. At the needle and the opposite electrode, other regular carbon structures, called carbon microflowers of high specific surface area, were also synthesized. Spectral analysis indicated that the carbon microstructures comprised about 89.9 at.% of elemental carbon. The structure of these products is partially crystalline and partially amorphous. The advantage of the method used is its low energy consumption. The mean power of the discharge is only 1 – 6 W.

References

[1] ZHU Y. Q. et al., *J. Mater. Chem.* 8, (1998), No.8, 1859-1864

[2] ZHU Y. Q. et al., *Adv. Mater.* 11, (1999),. No. 10, 844-847

[3] SHI E., CHO C.R., JANG M.S., JEONG S.Y., KIM H.J., *J. Mater. Res.* 9, (1994), No.11, 2914-2918

[4] MUKHOPADHYAY K., RAO K.U.B., *Adv. Sci. Lett.* 3, (2010), 486-490

[5] MORENO-COURANJOU M., MONTHIOUX M., GONZALEZ-AGUILAR J., FULCHERI L., *Carbon* 47, (2009), 2310-2321

[6] LISI N., GIORGI R., RE M., DIKONIMOS T., GIORGI L., SALERNITANO E., GAGLIARDI S., TATTI F., *Carbon* 49, (2011), 2134-2140

[7] THONGTEM S., SINGJAI P., THONGTEM T., PREYACHOTI S., *Mater. Sci. Eng.* A423, (2006), 209-213

[8] DENG J., ZHANG L., ZHANG B., YAO N., *Thin Solid Films* 516, (2008), 7685-7688

[9] KRIVCHENKO V. A. et al., *Carbon* 50, (2012), 1477-1487

[10] CHARINPANITKUL T., KANJANAPRAPAKUL K., LEELAVIWAT N., KURUKITKOSON N., KIM K.-S., *J. Ind. Eng. Chem.* 16, (2010), 912-917

[11] MA X., YUAN B., *Appl. Surf. Sci.* 255, (2009), 7846-7850

[12] ZHANG Q., HUANG J.Q., ZHAO M.Q., QIAN W.ZH., WANG Y., WEI F., *Carbon* 46, (2008), 1152-1158

[13] DU J., LIU ZH., LI ZH., HAN B., SUN ZH., HUANG Y., *Mater. Lett.* 59, (2005), 456-458

[14] GHOSH S., RAJ C.R., *J. Phys. Chem.* 114, (2010), No.24, 10843-10849

[15] SU L.A., JIA W.Z., ZHANG L.C., BEACHAM C., ZHANG H., LEI Y., *J. Phys. Chem. C* 114, (2010), No.42, 18121-18125

[16] ZHANG R.X., FAN L.Z., FANG Y.P., YANG S.H., *J. Mater. Chem.* 18, (2008), No.41, 4964-4970

[17] SOBCZYK A.T., JAWOREK A., *Acta Physica Polonica A*, 116, (2009), Suppl. 1, 136-138

[18] SOBCZYK A.T., JAWOREK A., RAJCH E., SOZAŃSKA M., *Solid State Phenomena* 140, (2008), 103-108

[19] SOBCZYK A.T., JAWOREK A., SOZAŃSKA M., *Journal of Electrostatics* 67, (2009), No.2-3, 275-279

[20] GARSCADDEN A., GANGULY B.N., HAALAND P.D., WILLIAMS J., *Plasma Sources Sci. Technol.* 3, (1994), 239-245

[21] BUDAEV V.P., KHIMCHENKO L.N., *Physica A* 382, (2007), 359-377

[22] GARSCADDEN A., *Pure & Appl. Chem.* 66, No. 6, (1994), 1319-1326

[23] TESSONNIER J.-P. et al., *Carbon*, 47, (2009), 1779-1798

[24] SLOVETSKY D. I., *Pure & Appl. Chem.*, 60, (1988), 753-768

[25] CHUANG A.T.H., BOSKOVIC B.O., ROBERTSON J., *Diamond Related Mater.* 15, (2006), 1103-1106

[26] DONNET J.B., OULANTI H., HUU T.L., *Diamond Related Mater.* 17, (2008), 1506-1512

[27] MA H.L., SU D.SH., KLEIN-HOFFMANN A., JIN G.Q., GUO X.Y., *Carbon* 44, (2006), 2254-2260

[28] QIU J., LI Y., WANG Y., *Carbon* 42, (2004), 2359-2362

[29] SHARMA CH.S., KULKARNI M.M., SHARMA A., MADOU M., *Chem. Eng. Sci.* 64, (2009), 1536-1543

[30] SHIH W.CH., JENG J.-M., HUANG CH.-T., LO J.-T., *Vacuum* 84, (2010), 1452-1456

[31] TANG J., JIN G.-Q., WANG Y.-Y., GUO X.-Y., *Carbon* 48, (2010), 1545-1551

[32] WANG J., ZHU M., OUTLAW R.A., ZHAO X., MANOS D.M., HOLLOWAY B.C., *Carbon* 42, (2004), 2867-2872

[33] WANG Z., SHOJI M., OGATA H., *Applied Surface Science* 257, (2011), 9082-9085

[34] XIAO Y., LIU Y., CHENG L., YUAN D., ZHANG J., GU Y., SUN G., *Carbon* 44, (2006), 1589-1591

[35] XU L., LIU J., DU J., PENG Y., QIAN Y., *Carbon* 43, (2005), 1560-1562

Received 2012-03-07
Accepted 2012-05-03